Response to Editor Comments

Dear editor,

Thank you for your effort on the article and for considering our manuscript for review.

We have modified the manuscript according to your comments. The "Data availability" section has been updated at the end of the manuscript.

Line 300-305:

Data Availability Statement

Data and code are available at Zenodo: https://doi.org/10.5281/zenodo.15827786. The repository includes the processed datasets and Python scripts necessary to reproduce the figures and results presented in this paper. Access requests of raw data can be submitted to http://124.70.110.235:9091/SubPlat_ChengDu/.

We appreciate your guidance and look forward to the next steps in the review process.

Best regards,
Pingyi Dong
on behalf of all co-authors

Response to Reviewer 1

We appreciate the time and effort that you devoted to reviewing our manuscript and are grateful for the insightful comments on improvements to our paper. We have revised the manuscript accordingly. Below, we provide a point-by-point response to each comment.

Point 1： All symbols and acronyms should be defined.

Thank you for the comment. We have corrected the errors in the manuscript. The revised sentence is in italics.

1.1 For frequencies of common weather radars.

Line 45-50: However, the precipitation intensity and the size of raindrops in the eastern Tibetan Plateau are relatively small compared to those in the middle and lower reaches of the Yangtze River (Pu et al., 2021), and the sensitivity of common weather radars to small particles is limited at their operating frequencies.

1.2 Define \lambda and \mu. (DSD formula probably needs to defined first.); the expansion of "GSD?"

Line 60-65: Due to the limited information obtained from single-frequency radar, the methods for retrieval

of DSD parameters are generally chosen to fix the μ parameter of the Gamma Size Distribution (GSD) (Kumar et al., 2011), or utilize λ-μ empirical relationships of GSD to constrain the retrieval results (Huang et al., 2021). In which, μ, and λ are shape, and slope parameters of GSD, respectively.

1.3 Need to define the terms! For example, what is \lambda here? What is Q_b?

Line 60-65: Where the efficiency factor of scattering (Q_b), backscattering section of radar (σ_b), extinction cross-section (σ_e) and $|K|^2$ are calculated by pyQuickBeam (Haynes et al., 2007).

1.4 Is the correction term in eq. (7). a polynomial fit in height based on Table 2 of Atlas et al. (1973)? If so, please state so.

Line 105-110: In Eq. 6, V(D) is the final falling velocity of raindrops considering the correction term of altitude h, which is calculated from Eq.7 (Atlas et al., 1973).

1.5 The observation uncertainties in ~~the~~ Z, Vr, and LDR are 0.5 dBZ, 0.5 m/s, and 0.5 dB, respectively.

Line 125-130: The observation uncertainties in Z, Vr, and LDR are 0.5 dBZ, 0.5 m/s, and 0.5 dB, respectively.

1.6 Which temperature lapse rate?

Line 155-160: The temperatures at different range gates of the radar are calculated using the temperature lapse rate. The temperature lapse rate is set to 6.5 ℃/km (Kattel et al., 2015).

1.7 What does "stratified" mean in this context?

Line 195-200: To validate the effectiveness of the optimal estimation algorithm, a random stratified sampling of 1800 cases of DSD is selected from the historical observations of the ground-based disdrometers. The precipitation cases were stratified according to the distribution range of N_0 and D_m, and 900 cases were sampled for each of the two parameters to ensure that the validation data covered a relatively comprehensive precipitation scenario.

1.8 You might want to spell this out at least once. CST can also stand for the Central Standard Time of the US.

Line 225-230: The precipitation events occurred from China Standard Time (CST) 00:00 to 08:12 and from CST 10:08 to 12:04, totaling 517 minutes.

Point 2： A few sentences are missing a verb..

Thank you for the comment. We have corrected the errors in the manuscript.

Line 115-120: This sentence is missing a verb.

The majority of D_m is less than 1.7

Point 3： We need to provide the necessary details, e.g., the polynomial (in h) correction in eq. (7).

Thank you for the comment. We have corrected the errors in the manuscript.

Line 105-110: In Eq. 6, V(D) is the final falling velocity of raindrops considering the correction term of altitude h, which is calculated from Eq.7 (Atlas et al., 1973)

Point 4： This is expected. How about the liquid water content? Is it approximately constant?

Thank you for the comment. The plot and discussion on RWC have been added to the article. Since the RWC is related to the 3-th moment of DSD, it increases as the rain intensity increase and exceeds on average about 0.2 g/m³ at strong echoes (30–45 dBZ).

Line 110-120: The calculated Z values are categorized into four intervals: [-10,10), [10, 20), [20, 30), and [30, 45). The $\log_{10}(N_0)$, D_m and Rain Water Content (RWC) in each Z interval are counted separately and illustrated in Figure1. RWC is calculated by, $\mathrm{RWC} = \frac{\pi}{6} \times 10^{-4} \int_{D\min}^{D\max} N(D) D^3 \mathrm{d}D$ *·*

Approximately 113000 samples of DSD are collected. The results show that the distribution of the $\log_{10}(N_0)$ ranges from 1.0 to 5.6. The majority of D_m is less than 1.7 mm. The statistical results indicate that as the Z of precipitation increases, the proportion of larger raindrops of DSD rises, and the concentration of raindrops decreases. Since the RWC is related to the 3-th moment of DSD, it increases as the rain intensity increase and exceeds on average about 0.2 g/m³ at strong echoes (30–45 dBZ).

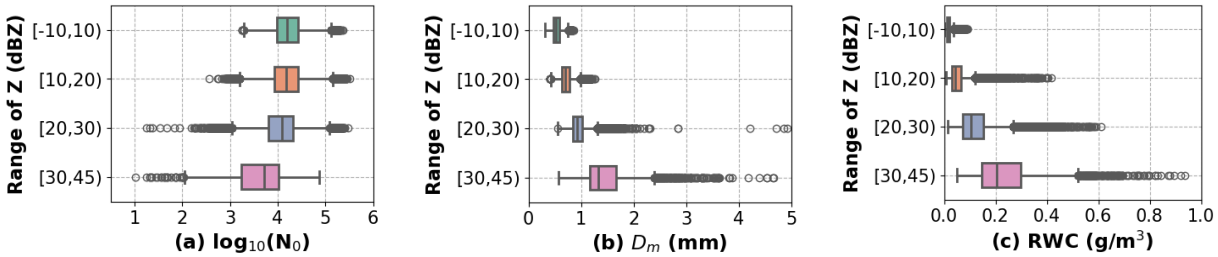

Figure 1. Box plots of the parameters of MP size distribution in different Z intervals. (a) $\log_{10}(N_0)$. (b) D_m. (c) RWC.

Point 5： It appears that extinction (and backscatter) efficiency is calculated using a temperature-dependent index of refraction m≡m(T), but the dielectric factor K, which also depends on m, is kept as a constant, i.e., no temperature dependency. Within 0-10 °C, |K|2 (used in calculating Z) has a ~2% variation, considerably smaller than the variation of m in the same temperature range. Is this the reason that a constant |K|2 is assumed?

Line 105; 190; 220-225: Thank you for the comment. When we verified the radar forward calculation, the dielectric constant of the Quickbeam script was set to the default value, the value for 35 GHz band radar is 0.88. We have corrected the error. We modified the scripts and reran the calculations. The calculated value of $|K|^2$ at 287.15 K is 0.903. In section 3.2, as shown in the modified Fig. 3, The The ME of Z is decreased from 3.63 to 3.48. In section 3.2, as shown in the modified Fig. 5, the JSD values of the retrieved D_m and the distribution of the observations of the ground-based disdrometer decreased 0.01. Other minor changes in the results are not reflected in the plotted figures.

Point 6： The extinction efficiency Q_e) is calculated using temperature dependent m

\equiv m(T). Why is the square of the dielectric factor |K|^2 kept at a constant 0.88 (Eq. 5)? Doesn't this introduce inconsistency? It may also be a cause to the difference between calculated and observed Z, right?

Line 105; 190; 220-225: Thank you for the comment. When we verified the radar forward calculation, the dielectric constant of the Quickbeam script was set to the default value, the value for 35 GHz band radar is 0.88. We have corrected the error. We modified the scripts and reran the calculations. The calculated value of $|K|^2$ at 287.15 K is 0.903. In section 3.1, as shown in the modified Fig. 3, The The ME of Z is decreased from 3.63 to 3.48. In section 3.2, as shown in the modified Fig. 5, the JSD values of the retrieved D_m and the distribution of the observations of the ground-based disdrometer decreased 0.01. Other minor changes in the results are not reflected in the plotted figures.

Point 7： Blue on black (Figure 5) is difficult to see. Consider using a lighter color than the blue used.

Thank you for the comment. We have redrawn the figure to improve its clarity.

Line 220-225:

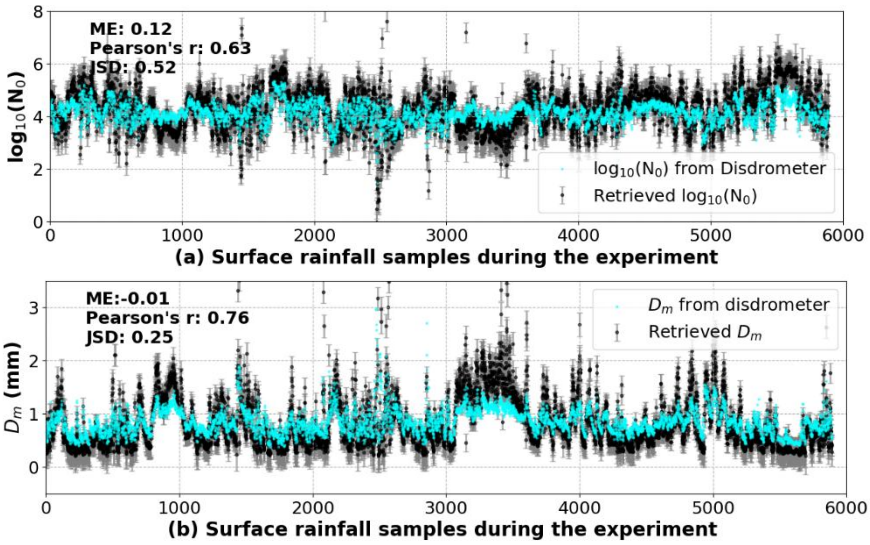

We hope that the revised version meets the requirements, and looking forward receiving your further comments and suggestions.

Response to Reviewer 2

We appreciate the time and effort that you devoted to reviewing our manuscript and are grateful for the insightful comments on improvements to our paper. We have revised the manuscript accordingly. Below, we provide a point-by-point response to each comment.

Point 1： Line 100: Should note that the velocity given is the Doppler Velocity since it is weighted by the backscatter cross section.

Thank you for the comment. We have revised it in the manuscript.

Line 100: For Ka-band radar, the reflectivity factor Z and the Doppler radial velocity Vr are calculated from Eq. (5) and (6).

Point 2： Line 104: Does the Haynes et al. algorithm account for the flattening of raindrops as they fall? This would certainly influence the details of the retrievals for heavier rain.

Thank you for the comment. The algorithm treats liquid hydrometeors as spheres and computes their scattering properties using Mie theory. Thus, the algorithm does not explicitly account for the oblateness (flattening) of raindrops as they fall. We agree that for large drops become more oblate [1]. *Yet, in our dataset most precipitations fall in the light to moderate rain regime, the contribution of very large drops is limited. To make this assumption and its implications explicit, we have revised the manuscript and now clarify.*

Line 304: In addition, the retrievals performance and microphysical characteristics under intense convective conditions are not considered, and raindrops are assumed to be spherical in the radar forward model. Further research is necessary regarding retrievals assumptions in these scenarios with Ka-band zenith-pointing radar, such as the treatment of raindrop shape and DSD parameterizations in the retrieval.

[1] E. A. Brandes, G. Zhang, and J. Vivekanandan, "Experiments in rainfall estimation with a polarimetric radar in a subtropical environment," *Journal of Applied Meteorology,* vol. 41, no. 6, pp. 674-685, 2002.

Point 3： Line 133: It would be useful to see examples of the covarinace matrices or frequency distribution plots of the terms in Sa.

Thank you for the comment. We have now added a figure about the frequency distribution of the prior database, a heatmap of Sa, and a description of prior information in the manuscript.

Line 135: The observational vector y_{obs} of the optimal estimation algorithm consist of the Z and V_r observed by the Ka-band zenith-pointing radar, and the state vector x comprises $log_{10}(N_0)$ and D_m. The first guess of x_a, and the priori error covariance matrix S_a are set based on the prior information of the DSD in Hongyuan. From the precipitation cases described in section 2.1, a subset of 6680

case is selected to construct the prior dataset. The dataset is obtained by stratified random sampling based on the calculated Z. This approach reduces the over representation of frequent weak precipitation samples in the prior and yields a more uniformly distributed and representative priori dataset (Boschetti et al., 2016). Then, the values of D_m are normalized since the state vector are assumed to be approximately Gaussian in optimal estimation, and statistical analysis of the dataset shows that the distribution of D_m departs from normality. After the transformation, the prior database for the retrieval is established. The mean value of $log_{10}(N_0)$ and D_m in the dataset is set as the first guess x_a for the retrieval. The frequency distribution of $log_{10}(N_0)$ and normalised D_m are plotted in Figure 2 (a). S_a calculated from the database are plotted in Figure 2 (b).

Boschetti, L., Stehman, S. V., and Roy, D. P.: A stratified random sampling design in space and time for regional to global scale burned area product validation, Remote sensing of environment, 186, 465-478, 2016.

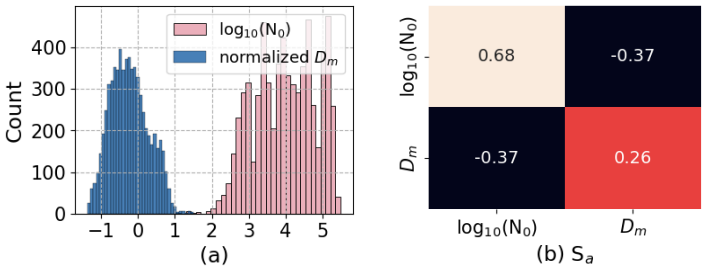

Figure 2. The frequency distribution of the prior database and the heatmap of S_a used in the retrieval. (a) Frequency distribution of N_0 and normalized D_m, and (b) heatmap of S_a.

Point 4： Line 133: Is the covariance matrix constant or is there a state dependent Sa? Are the terms considered to be correlated?

Thank you for the comment. In this study, we use a constant, state-independent covariance matrix S_a for all retrievals. The the off-diagonal terms of S_a are retained, which represent the priori covariance between N_0 and D_m. The statistics results of the two parameter has correlation, and using a full S_a preserves this physically meaningful relationship in the prior. We have added a description in the paper.

Line 144: In the study, the S_a is a constant matrix, and includes correlations between N_0 and D_m derived from the prior database.

Point 5： Line 134: Additional information should be provided regarding the observational error covariance matrix. Are the errors considered correlated or uncorrelated. What is the source of the uncertainty?

Thank you for the comment. The observational vector is assumed uncorrelated and S_y is specified as a constant diagonal matrix. The observation uncertainty is 0.5 and 0.5 m/s for Z and V_r, respectively. The value on the diagonal of the matrix is the squire of observation uncertainty. We have added descriptions on the retrieval method.

Line 148: The measurement of Z and V_r is assumed to be uncorrelated, and the value on the diagonal of the matrix is squire of the observation uncertainty.

Point 6： Line 137: There needs to be more information regarding how the terms of Jacobian, Kx, are calculated and please provide typical examples of the values of Kx. These details are useful because they show the degree to which the quantities to be retrieved are sensitive to the observations used to constrain them.

Thank you for the comment. The Jacobian matrix K_x is defined as $\mathrm{K_x}=\frac{\delta \mathrm{F(x)}}{\delta \mathrm{x}}$. *We compute the elements of K_x numerically by finite differences around the current state at each iteration of the retrieval,* $\mathrm{K_x}=\frac{\delta \mathrm{F(x)}}{\delta \mathrm{x}} \approx \frac{\mathrm{F(x+\partial x)-F(x)}}{\partial \mathrm{x}}$. *In which, ∂x is a perturbation chosen as 1% for each iterated state vector. we have added a typical example of the values of K_x in the manuscripts. The typical value of K_x indicate that the Z is sensitive to both $log_{10}(N_0)$ and D_m, with $\partial Z/\partial log_{10}(N_0)$ and $\partial Z/\partial D_m$ on the order of 10 and 20, respectively. And V_r is almost insensitive to $log_{10}(N_0)$ and only affected by D_m, with $\partial V_r/\partial log_{10}(N_0) \approx 0$ and $\partial V_r/\partial D_m \approx 2.3$. This pattern indicates that the mainly constrains the retrieval of N_0 and D_m, while V_r provides complementary sensitivity to D_m.*

Line 48: Where K_x represents the Jacobian matrix computed at the x-th iteration. The elements of K_x numerically computed by finite differences around the state vector at each iteration of the retrieval, the perturbation is chosen as 1% of the state vector. The typical value of K_x indicate that the Z is sensitive to both $log_{10}(N_0)$ and D_m, with $\partial Z/\partial log_{10}(N_0)$ and $\partial Z/\partial D_m$ on the order of 10 and 20, respectively. And V_r is almost insensitive to $log_{10}(N_0)$ and only affected by D_m, with $\partial V_r/\partial log_{10}(N_0) \approx 0$ and $\partial V_r/\partial D_m \approx 2.3$. This pattern indicates that the mainly constrains the retrieval of N_0 and D_m, while V_r provides complementary sensitivity to D_m.

Point 7： Figure 3: The authors should comment on the cause and influence of the systematic biases between the forward calculation and the observations that show up in this plot. the explanation given regarding the height difference and wind may be reasonable but how those issues would result in the biases shown should be demonstrated.

The fact that the calculated values do not lie on the 1:1 line suggest that there may be forward model errors that are not accounted for - i.e. the assumption of spherical raindrops versus reality. Accounting for forward model errors is key in these types of OE inversions. Very often the forward model errors are larger (usually significantly larger) than the uncertainties in the observations.

Thank you for the comment. In the revised manuscript we provide a more detailed discussion of the systematic differences between the forward-calculated and observed quantities of radar. In section 3.1, we added the discussion on forward model errors.

This bias is possibly due to differences in the sampling volumes of the radar and disdrometer, since the disdrometer measures the raindrop at surface and the first effective range bin of radar is at 210m. Besides, the wind at the surface may influence the accuracy of the measurements of the disdrometer. Furthermore, as the raindrops fall, they may deviate from the spherical shape assumption in the radar forward model, leading to discrepancy between the forward simulation and observed values.

In section 3,2, we added a discussion on the retrieved and observed $\log_{10}(N_0)$ and D_m during the field campaign in July and August 2024.

The bias between the retrieved and observed parameters of DSD may be attributed to the observation uncertainties and the differences in the sampling volumes of the two instruments, as well as errors introduced during the fitting of parameters from DSD. More importantly, based on the validation of the radar forward calculation, there is a bias between the radar observation and simulation. Physical assumptions in the scattering calculations, such as the spherical-drop approximation, may also contribute to discrepancies between the retrieved values and the surface DSD parameters.

Line 98: This bias is possibly due to differences in the sampling volumes of the radar and disdrometer, since the disdrometer measures the raindrop at surface and the first effective range bin of radar is at 210m. In addition, the wind at the surface may influence the accuracy of the measurements of the disdrometer. Furthermore, as the raindrops fall, they may deviate from the spherical shape assumption in the radar forward model, leading to discrepancy between the forward simulation and observed values.

Line 230: The bias between the retrieved and observed parameters of DSD may be attributed to the observational uncertainties and the differences in the sampling volumes of the two instruments, as well as errors introduced when fitting the DSD parameters. More importantly, based on the validation of the radar forward calculation, there is a bias between the radar observation and simulation. Physical assumptions in the scattering calculations, such as the spherical-drop approximation, may also contribute to discrepancies between the retrieved values and the surface DSD parameters.

Point 8: Figure 4 and 5: Should explain the meaning of the error bars in figures 4 and 5. How are they derived?

Thank you for the comment. We have added descriptions on the retrieval method. The revised sentence is in italics.

Line 45-50: S_x in Eq. (11) provides the uncertainty of the retrieved x_x:

$$S_x = (S_x^{-1} + K_x^T S_y^{-1} K_x)^{-1} \quad (11)$$

If the convergence of retrieval is achieved, the x_x and S_x are the optimal solution x_{op} and corresponding uncertainty S_{op}

Line 213 The final value of S_x after retrieval convergence is indicated by error bar in the figure.

Point 9： Line 221: The contention made by the authors that N0 is higher and Dm smaller at the melting layer is not obvious in the data shown. If the authors think this is important, they should devise a way of showing it more clearly.
Thank you for the comment. We mean value of N_0 and D_m are calculated for the lighter and heavier rain, and added a description in the paper.

Line 246: Based on the statistic results of lighter rain (maximum value of Z under 30 dBZ) and heavier rain (maximum value of Z exceed 30 dBZ) in this day, the retrieved profiles of $\log_{10}(N_0)$ suggest a higher raindrop concentration in the upper levels of precipitation. At top of the precipitation layer, the mean value $\log_{10}(N_0)$ is 5.3 for heavier rain and 4.7 for lighter rain, and the mean of D_m is 0.65 and 0.46 mm. For heavier rain, the vertical variation of the retrieved N_0 and D_m is larger compared to other precipitation samples, the mean absolute value of $(Z_{hi+1} - Z_h)/\Delta h$ is 0.01 for $\log_{10}(N_0)$ and 0.002 for D_m. For lighter rain, the value of $\log_{10}(N_0)$ and D_m is 0.009 and 0.001, respectively. Samples 480 to 500 occurred at the end of a brief rainfall in the morning. The maximum value of Z is below 20 dBZ. The retrieved profiles of $\log_{10}(N_0)$ were generally larger than those of other precipitation samples, while the retrieved profiles of Dm indicated smaller raindrop sizes.

Point 10： Line 242: I wonder if it would make sense to separate this into warm rain events versus cold? It seems likely that the Tsukuba results were associated with rain just below the melting layer when drops derived from large aggregate snow would begin to break up. That is not what is implied by Figure 7 of this paper.
Thank you for the comment. We agree that distinguishing between warm and cold rain events is important for the characteristic of DSD. A full separation of our statistics into warm and cold rain events would indeed be valuable. Yet this would require accurate classification of each profile and co-located thermodynamic information, which is beyond the scope of the present paper. We have added a paragraph in the discussion to acknowledge this limitation.

Line 302: The DSD characteristic of warm and cold rain is an important topic, since it relates to distinct microphysical process. The classification of warm and cold rain event and their DSD characteristic should be studied in future work.

In the paper by Tsukuba et al., they refer that some single giant raindrops are observed just below the melting layer. Using this result to compare with the retrieved D_m parameter here is inappropriate. We have revised this part.

Line 269: The mean D_m for heavy precipitation is generally larger than lighter precipitation, and

increases as the raindrops fall, reaching a peak at around 0.5 km. This may relate to the equilibrium of coalescence and breakup effects of raindrops during their falling process (Gatlin et al., 2018).

Gatlin, P. N., Petersen, W. A., Knupp, K. R., and Carey, L. D.: Observed response of the raindrop size distribution to changes in the melting layer, Atmosphere, 9, 319, 2018

Point 11： Figure 8: Explain the meaning of the box plot. i.e. Median, Interquartile, 90'th, and 10'th percentiles?

Thank you for the comment. The central line in each box indicates the median, and the bottom and top edges of the box indicate the 25th and 75th percentiles of the parameters. We have added descriptions on the box plot. The revised sentence is in italics.

Line 253: In the box plot, the central line of each box indicates the median, and the box edges indicate the lower and upper quartiles of the parameters.